AD-A174 783 PASSIVE Q-SWITCHING OF CO2 TEA LASER USING SULFUR HEXAFLUORIDE (SF6)(U) NIGHT VISION AND ELECTRO-OPTICS CENTER FORT BELVOIR VA R PASTEL OCT 86 1/1

UNCLASSIFIED AMSEL-NV-TR-0056 F/G 20/5 NL

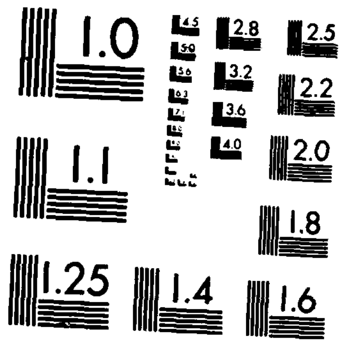

ICROCOPY RESOLUTION TEST CHART
NATIONAL BUREAU OF STANDARDS-1963-A

2

Center for Night Vision and Electro-Optics

AMSEL-NV-TR 0056

PASSIVE Q-SWITCHING OF CO_2 TEA LASER USING SULFUR HEXAFLUORIDE (SF_6)

by
Robert Pastel

October 1986

Approved for public release; distribution is unlimited.

FORT BELVOIR, VA 22060-5677

UNCLASSIFIED

SECURITY CLASSIFICATION OF THIS PAGE

AD-A174783

REPORT DOCUMENTATION PAGE

1a. REPORT SECURITY CLASSIFICATION UNCLASSIFIED	1b. RESTRICTIVE MARKINGS
2a. SECURITY CLASSIFICATION AUTHORITY	3. DISTRIBUTION/AVAILABILITY OF REPORT Approved for public release; Distribution is unlimited.
2b. DECLASSIFICATION/DOWNGRADING SCHEDULE	
4. PERFORMING ORGANIZATION REPORT NUMBER(S) Report AMSEL-NV-TR-0056	5. MONITORING ORGANIZATION REPORT NUMBER(S)
6a. NAME OF PERFORMING ORGANIZATION CENTER FOR NIGHT VISION & ELECTRO OPTICS; 6b. OFFICE SYMBOL (If applicable) AMSEL-RD-NV-L	7a. NAME OF MONITORING ORGANIZATION
6c. ADDRESS (City, State, and ZIP CODE) FORT BELVOIR RD&E CENTER FORT BELVOIR, VA 22060-5077	7b. ADDRESS (City, State, and ZIP CODE)
8a. NAME OF FUNDING/SPONSORING ORGANIZATION CNVEO; 8b. OFFICE SYMBOL	9. PROCUREMENT INSTRUMENT IDENTIFICATION NUMBER
8c. ADDRESS (City, State, and ZIP CODE) FORT BELVOIR, VA 22060-5077	10. SOURCE OF FUNDING NUMBERS: PROGRAM ELEMENT NO. / PROJECT NO. / TASK NO. / WORK UNIT ACCESSION NO.

11. TITLE (Include Security Classification)

PASSIVE Q-SWITCHING OF CO_2 TEA LASER USING SULFUR HEXAFLUORIDE (SF_6)

12. PERSONAL AUTHOR(S) ROBERT PASTEL

13a. TYPE OF REPORT	13b. TIME COVERED	14. DATE OF REPORT (Year, Month, Day)	15. PAGE COUNT
LAB RESULTS	FROM 4/86 TO 8/86	October 1986	

16. SUPPLEMENTARY NOTATION

17. COSATI CODES			18. SUBJECT TERMS (Continue on reverse if necessary and identify by block number)
FIELD	GROUP	SUB-GROUP	Passive Q-switching; CO_2 TEA Laser; Sulfur Hexafluoride

19. ABSTRACT (Continue on reverse if necessary and identify by block number)

Passive Q-switching of CO_2 TEA laser using sulfur hexafluoride (SF_6) has been demonstrated at 10.2 μm. There is minimum loss of peak power, narrowing of the pulse, and elimination of the tail. Q-switching at 9.6 μm is not observed. Also discussed is the use of SF_6 to frequency the laser to the strong gain lines of the 10.2 μm and 9.6 μm branch of the CO_2 emission. Both theory and experimental results are given.

20. DISTRIBUTION/AVAILABILITY OF ABSTRACT ☐ UNCLASSIFIED/UNLIMITED ☐ SAME AS RPT. ☐ DTIC USERS	21. ABSTRACT SECURITY CLASSIFICATION
22a. NAME OF RESPONSIBLE INDIVIDUAL	22b. TELEPHONE (Include Area Code); 22c. OFFICE SYMBOL

DD FORM 1473, 84 MAR

83 APR edition may be used until exhausted.
All other editions are obsolete.

UNCLASSIFIED

SECURITY CLASSIFICATION OF THIS PAGE

Table of Contents

Figures

Tables

Passive Q-Switching of CO_2 TEA Laser Using Sulfur Hexafluoride

I. Introduction

The use of an infrared-absorbing gas such as sulfur hexafluoride (SF_6) to passively Q-switch a low pressure carbon dioxide (CO_2) laser operating at a wavelength of 10.6 microns (μm) has been extensively reported in literature (see references 1, 2, and 3, p. 14). Recent interest in using sulfur hexafluoride as a Q-switch for atmospheric pressure TEA lasers has been motivated by the need for an optimized laser for generation of the second harmonic of the CO_2 laser radiation.

Second harmonic generation is accomplished by directly pumping a crystal having favorable nonlinear optical properties with radiation from the primary laser source. Neglecting loss mechanisms, the second harmonic output is directly in proportion to the input power to the frequency doubling crystal. For this reason, when using a typical TEA laser as the pump source, second harmonic output is attributable primarily to the high-power, gain-switched spike of the input pulse. The substantial energy content in the relatively long, low-power tail of the pulse contributes little to the second harmonic output. Unfortunately, it also causes detrimental heating of the crystal.

Second harmonic output is limited by the energy density with which doubling crystals can be pumped without sustaining damage. Elimination of the tail of the laser pump pulse, therefore, can allow higher power pumping and higher second harmonic output without damage to the doubling crystal. Various means may be used to optically clip off the tail of the pulse. It would be desirable, however, to transfer the energy normally contained in the tail to the short, high-power spike. This would result in a more efficient, compact source for a given pump power.

Introduction of an absorbing gas into the laser cavity makes possible some degree of frequency tuning of the TEA laser. The selective absorption property of SF_6 makes it possible to change the lasing frequency of a free-running TEA laser (without grating) from 10.6 μm to 10.2 μm and from 10.2 μm to 9.6 μm as the SF_6 pressure is increased. Operation at 9.6 μm is desirable because the doubled output at 4.8 μm is inside the atmospheric transmission window of 3 to 5 μm. The second harmonic frequencies generated from 10.2 μm and 10.6 μm pump radiation are outside this band.

A Q-switched CO_2 laser may also be advantageous for other applications. For fast detection systems (15 MHz and faster) such as laser rangefinders, the use of a Q-switched laser can result in reduced noise and increased range. Sulfur hexafluoride has been used to demonstrate mode locking of CO_2 lasers (see references 4, 5, and 6, p.14), which may be used for high-range resolution requirements.

The ability of SF_6 to be used to frequency tune a CO_2 laser can be beneficial for applications requiring operation in other branches of the CO_2 emission spectrum. The absorbing gas offers a method to frequency tune with minimal loss and high reliability.

This report documents some of the above-cited properties when SF_6 is introduced into the laser cavity. The potential and the limitations of using absorbing gases for passive Q-switching are addressed, and an heuristic theory is given for passive Q-switching and frequency selection.

II. Theory

The basic mechanism of Q-switching refers to the modulation of the loss in a laser cavity in order to produce a high-power output pulse. A simple method of active Q-switching is to mount the rear reflector of the laser resonant cavity onto a rotating shaft. While the mirror is turned away from the cavity, the cavity loss is high and the population inversion of the laser medium can build up past its normal lasing threshold. When the rotating rear reflector becomes aligned with the output coupler, the cavity loss is lowered and the Q of the cavity is raised. The gain of the laser is extremely high causing a rapid build up of lasing to high peak powers (see reference 7, p.14).

The mechanism of passive Q-switching, using saturable absorbing gases, is more subtle. Several articles have presented models and theories of passive Q-switching (references 1 and 2). In brief, the inclusion of a saturable absorbing gas into the cavity introduces high loss to the cavity during the beginning of the excitation process and allows the population inversion to overshoot the normal threshold value. When the emission becomes strong enough to saturate the absorbing gas, the loss decreases and the inverted population quickly falls to its threshold value while simultaneously emitting at the laser frequency. This explanation of passive Q-switching points out two necessary properties of the saturable absorber used as a Q-switch: (1) it must be an effective absorber at the lasing frequency, and (2) it must have a metastable energy state near that of the lasing transition so that the absorber will become saturated. The pressure of the absorption cell must be controlled so that at some time the small signal absorption of the absorbing gas is lower than the gain vs. time profile of the laser (for lasing to occur). The relaxation time of the metastable state will determine the pulse length. References 8 and 9 on page 14 demonstrate that SF_6 is a good candidate for Q-switching at 10.6 μm. This paper will show that SF_6 also can be used as a passive Q-switch at 10.2 μm.

The difficulty of Q-switching a TEA laser is that the TEA laser is already strongly gain switched by the pulse-forming network of the discharge capacitor. But with a proper pressure of the absorbing gas, it may be possible to further delay the onset of the laser pulse, allowing an even larger overshoot of the population inversion. The absorbing gas can eliminate the tail of the laser pulse if it has recovered from saturation in time to absorb the tail's photon flux. This requires the relaxation time of the metastable state to be on the order of the pulse width and the absorbing gas pressure to be high enough to absorb all of the tail's photon flux.

There are three requirements on the pressure and length of the saturable absorbing gas cell for it to perform Q-switching and eliminate the tail of the pulse in a TEA laser:

1. The pressure must be high enough to induce short relaxation time but not so high that the relaxation time is shorter than the pulse width.
2. The pressure-length product must be high enough to appreciably delay lasing but not so high as to inhibit lasing.
3. The pressure-length product must be high enough to absorb all of the tail's photons.

The first requirement puts limits on the gas pressure while the second puts limits on the gas cell length. It may be impossible to achieve the third condition without invalidating the second.

The mechanism of frequency tuning a TEA laser, using absorbing gas, is a process of selective frequency absorption. From Figure 1, page 8, it is apparent that even at low pressures, SF_6 is very absorbent at 10.6 μm. At low pressures, the loss at 10.6 μm is too high to permit lasing, but the laser is free to lase at 10.2 μm where SF_6 is not absorbing. At higher pressures, SF_6 is also strongly absorbent at 10.2 μm, and lasing is inhibited at both 10.2 μm and 10.6 μ. The laser is, therefore, forced to lase at 9.6 μm where there is no appreciable absorption by SF_6.

III. Experiment

Three types of experiments were performed to demonstrate and explain the Q-switching and frequency-tuning behavior of SF_6 used intracavity. These were:

1. Passive Q-switching of a TEA laser with a 100-percent reflecting rear mirror and SF_6 inside the cavity.
2. Passive Q-switching of a TEA laser with a grating used to frequency tune and SF_6 inside the cavity.
3. Absorption spectrum of SF_6 in the 9 μm to 11 μm.

The first experiment was designed to demonstrate passive Q-switching and frequency tuning from 10.6 μm to 9.6 μm. The experimental layout is shown in Figure 2, page 9. The first SF_6 gas cell was constructed with a glass body and two zinc selenide (ZnSe) brewster windows and measured 27 cm along the axis. The gas cell was evacuated, then filled to operating pressures of from 1 to 100 torr of SF_6. The discharge was 45 cm long and was flowing at atmospheric pressure. The mixture of flowing gas was monitored at 5200 cc/min He, 3200 cc/min CO_2, and 500 cc/min N_2. A photon drag detector, Model 7401 from Rofin LTD, was used to measure pulse width and tail length.

The data collected from the experiment included total energy, lasing wavelength, and pulse shape at various pressures of SF_6. It was found that a trace amount of SF_6 inhibited lasing at 10.6 μm. Table 1 shows a summary of results.

Table 1. Passive Q-Switching With 27 cm Gas Cell

SF_6 pressure (torr)	Lasing Wavelength (μm)	Total Energy (milijoules)	Percent Peak Power	Pulse Shape
0	10.6	180	100	150 nsec pulse with 1 μsec tail
3-6	10.2	82	90	Q-switch 100 nsec pulse
11	9.6	93	70	100 nsec pulse with tail

Operating Conditions: 31 kv on capacitors
85% flat output coupler
4-meter rear reflector

The criterion for Q-switching was the disappearance of the tail with minimal loss of peak power. A pressure of 3 torr of SF_6 was found to consistently produce the best Q-switching at 10.2 μm, and 90 percent of the peak power was obtained with the laser operating at 10.6 μm with no SF_6. The listed percentages of total energy are energies compared to the output with the laser operating at 10.6 μm for that set of experiments. The energy was consistently 40 percent of the 10.6 μm pulse energy. This compares favorably with the assumption that roughly 50 percent of the energy in the 10.6 μm pulse is found in the tail. Slightly lower output would be expected for the lower gain 10.2 μm transition.

Transition of lasing from 10.2 μm to 9.6 μm was found to occur at a pressure of around 11 torr. The transition was not abrupt. A 1-2 torr lower pressure, lasing would occur simultaneously at 9.6 μm and 10.2 μm. Operation of the laser at 9.6 μm was not nearly as consistent as operation at 10.2 μm. The pulse shape would vary from pulses with very small tails to double pulsing. The peak power of the 9.6 μm pulse was down 50 percent from that of the 10.6 μm pulse. The pulse shapes of laser pulse for the three operating regions are shown in Figure 3 on page 10.

The experiment then was repeated with a gas cell 60 cm in length. A summary of the results is shown in Table 2.

Table 2. Passive Q-Switching With 60 cm Gas Cell

SF_6 pressure (torr)	Lasing Wavelength (μm)	Total Energy (milijoules)	Percent Peak Power	Pulse Shape
0	10.6	135	100	300 nsec pulse, 1 μsec tail
1.4-5	10.2	80	30	175 nsec pulse, small tail
6	9.6	55	3	100 nsec pulse, 800 nsec tail

Operating Conditions: 31 kv on capacitors
85% flat output coupler
4-meter rear reflector

The results for the longer gas cell show the transitions to 9.6 μm occurring at 6 torr SF_6, approximately half the SF_6 pressure as for the shorter cell. Optimal Q-switching at 10.2 μm lasing occurred at 1.5 torr SF_6. All the pulses were wider than for the short cell due to the increased length of the resonant cavity. Effective Q-switching of the 9.6 μm laser pulse still was not observed. Figure 4 (page 11) shows the pulse shapes for the three operating regions.

A major failure of the above experiment was that the 10.6 μm laser pulse was used as the baseline for comparison of the 10.2 μm and 9.6 μm lasing pulse and for the determination of Q-switching. A second experiment was devised, replacing the rear mirror with a grating. The laser was then tuned to the strongest line of the 10.6 μm, 10.2 μm, and 9.6 μm branches of the CO_2 laser. The SF_6 gas cell pressure was varied, and the same measurements were taken. The reader is cautioned not to try to compare pulse height and total energy of different wavelengths because both the laser and the photon drag detector were realigned for each change of wavelength. Table 3 shows the results of this experiment.

Table 3. Passive Q-Switching With Grating

Laser Line	SF_6 Pressure (torr)	Percentage Total Energy	Percentage Peak Power	Pulse Shape
10P18	0	100	100	100 nsec pulse, 1 μsec tail
10P18	.3	0	0	No lasing
10P18	.1	0	0	No lasing
10R18	0	100	100	75 nsec pulse, 700 nsec tail
10R18	1	90	100	75 nsec pulse, 700 nsec tail
10R18	2.5	65	70	75 nsec pulse, 700 nsec tail
10R18	3.3	52	70	100 nsec pulse, no tail
10R18	6.0	30	42	100 nsec pulse, no tail
10R18	8.0	10	14	100 nsec pulse, no tail
9P16	0	100	100	75 nsec pulse, 500 nsec tail
9P16	20	90	83	75 nsec pulse, 500 nsec tail
9P16	40	68	66	75 nsec pulse, 200 nsec tail
9P16	70	36	50	75 nsec pulse, 200 nsec tail

Operating Conditions: 31 kv on capacitor
90% flat output coupler
160 lines/mm grating

The percentage of peak power and total energy are ratios made to the output with the cell empty for the corresponding gas cell pressures at that wavelength. With the laser tuned to the 10 μm-P18 line, it was found that any amount of SF_6 quenched the lasing. The results at 10 μm-R18 are more interesting, and the corresponding scope traces display vividly the Q-switching at 10.2 μm. Q-switching occurs around 3 torr SF_6. The percentage of peak power is lower than in the previous experiment without the grating, and the pulse width is greater. This is probably due to the increased cavity length and loss required to introduce the grating into the cavity. The results for the 9 μm-P16 line showed no indication of Q-switching. The pulse did appear to change until 20 torr SF_6, after which it was progressively attenuated. The results with the grating confirmed the results achieved with a rear mirror and using the SF_6 to frequency tune the laser. Figure 5 (p. 12) shows the impulse shape for the three frequencies at various SF_6 pressure.

A third experiment was conducted to acquire the absorption spectrum of SF_6 in order to explain the results of the two previous experiments. Reference 10 gives high resolution absorption spectrum of SF_6 at 10.6 μm, but the spectrum does not extend to 10.2 and 9.6 μm. Gas samples of SF_6 at varying pressures were analyzed using two spectrophotometers. The gas cell used was 10 cm in length and bounded by two flat, uncoated potassium bromide (KBr) windows. Figure 1 shows the transmission spectrum of SF_6 with the 5MX Nicolet Fourier transform infrared (FT-IR) spectrophotometer. The resolution of the FT-IR is 4 wave numbers, and the traces represent an average of 10 scans. Because the gas cell used for the spectroscopy is about one third the length of the short gas cell used intracavity, one needs to divide the pressures by 3 to find the corresponding pressures and the transmission of the

intracavity cell. These sets of transmission spectra clearly demonstrate the frequency selectivity of SF_6. The 1 torr SF_6 curve shows that the 10.6 μm absorption of SF_6 is strong enough to inhibit lasing at 10.6 μm, while the 10.2 μm absorption is down to 5 percent, which will permit lasing at 10.2 μm. The 10 torr spectrophotometer curve represents the absorption at which Q-switching occurred at 10.2 μm. The absorption is appreciable (10-30 percent). Even from this 4-wave number resolution spectroscopy, one can observe that there is some structure to the absorption band of SF_6 at 10.2 μm. The 40 torr trace represents the point at which the laser is operating entirely at 9.6 μm. The transmission at 10.2 μm is down 30 percent, while the absorption of 9.6 μm is only 10 percent. It is at 300 torr that some structure is observed at 9.6 μm, although the absorption is still only 15 percent.

Because this absorption band at 9.6 μm only appears at high pressures, it is probably due to some secondary collosional process and is short lived. Short lifetime processes would not lead to Q-switching but rather to a loss to the laser. The molecules of SF_6 absorbing the photons would not accumulate into one state and thereby saturate. The second set of curves are from the Perker Elmer 9836 infrared spectrophotometer. The spectroscopy curves were run at 1- to 0.5-wave number resolution in order to observe the fine structure of the absorption spectrum. Although the curves in Figure 6 (p.13) contain quite a bit of noise, the structure at 10.6 μm and 10.2 μm is quite apparent. Attempts were made to process the data in order to find some structure at 9.6 μm, but none were achieved.

IV. Conclusion

It has been demonstrated that SF_6 can be used intracavity to frequency tune a TEA laser to the strong lines of the 10.2 μm and 9.6 μm branches of the CO_2 emission spectrum. It has also been shown that SF_6 can passively Q-switch the CO_2 TEA laser at 10.2 μm, although there was no indication of increased peak power to the gain switch spike. Consistent Q-switching at 9.6 μm was not observed. The absorption spectrum of SF_6 shows that Q-switching at 10.2 μm can be expected but does not give any support to Q-switching at 9.6 μm. The use of SF_6 intracavity to frequency tune and Q-switch at 10.2 μm is considered efficient because of its simplicity of installation and high reliability.

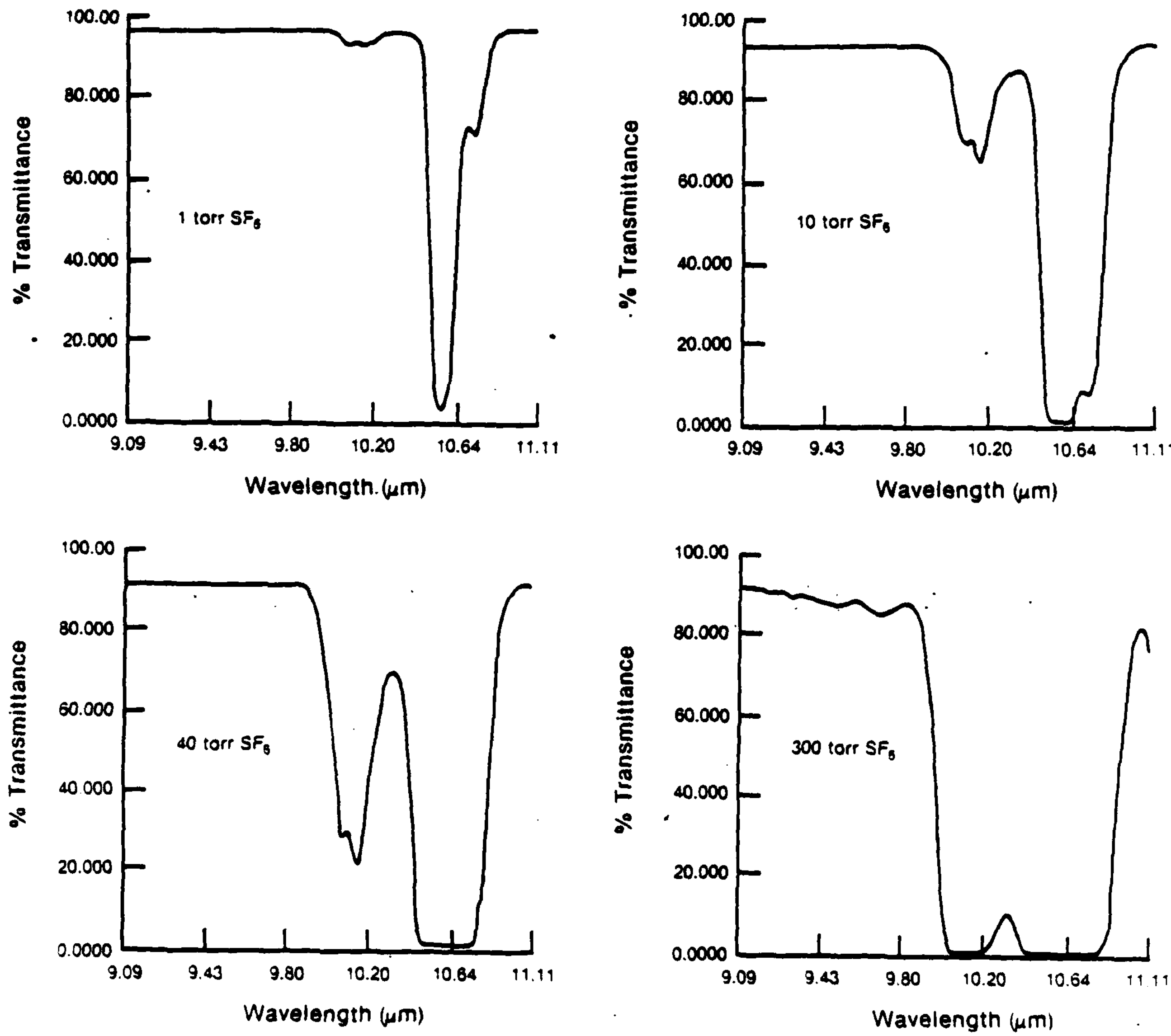

Figure 1: Transmission Spectrum of SF_6 From 5-MX Nicolet FT-IR

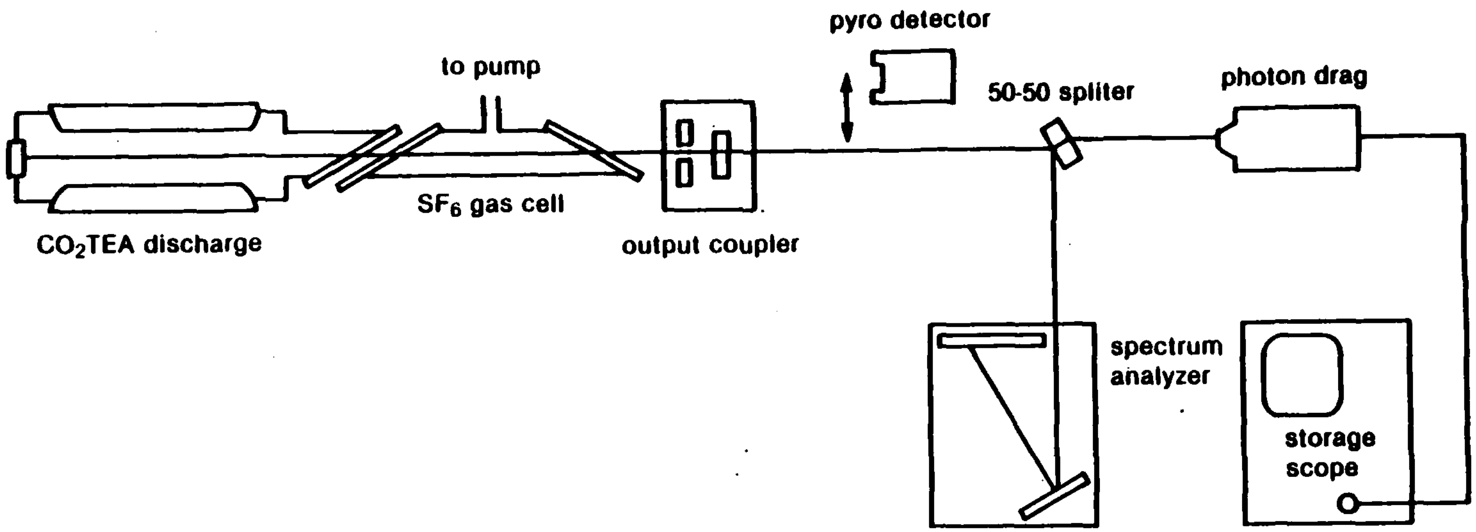

Figure 2: Optical Layout for Diagnostic of Passive Q Switch TEA Laser

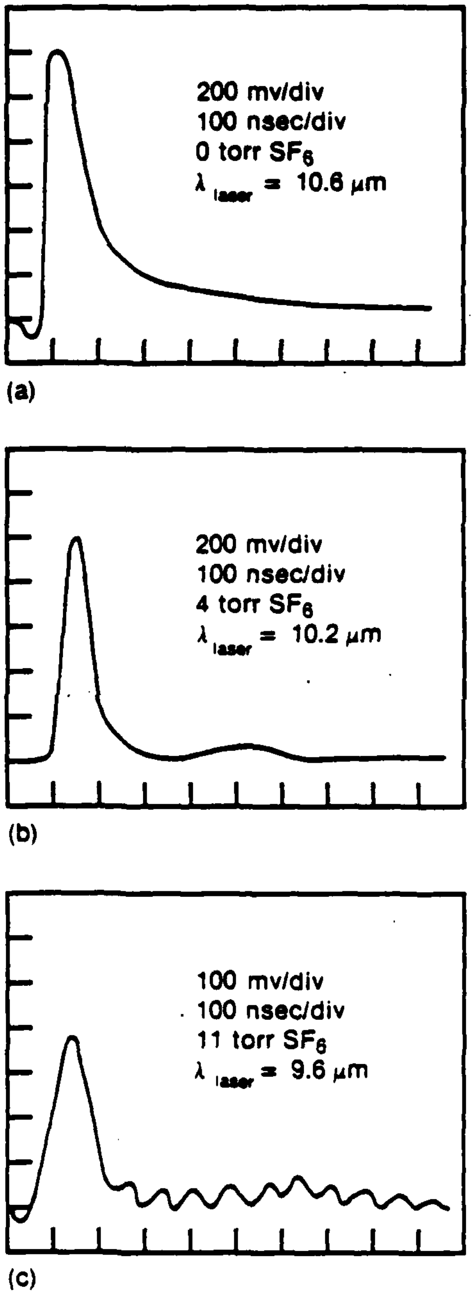

Figure 3: Scope Traces of Laser Pulse With 27cm SF_6 Gas Cell

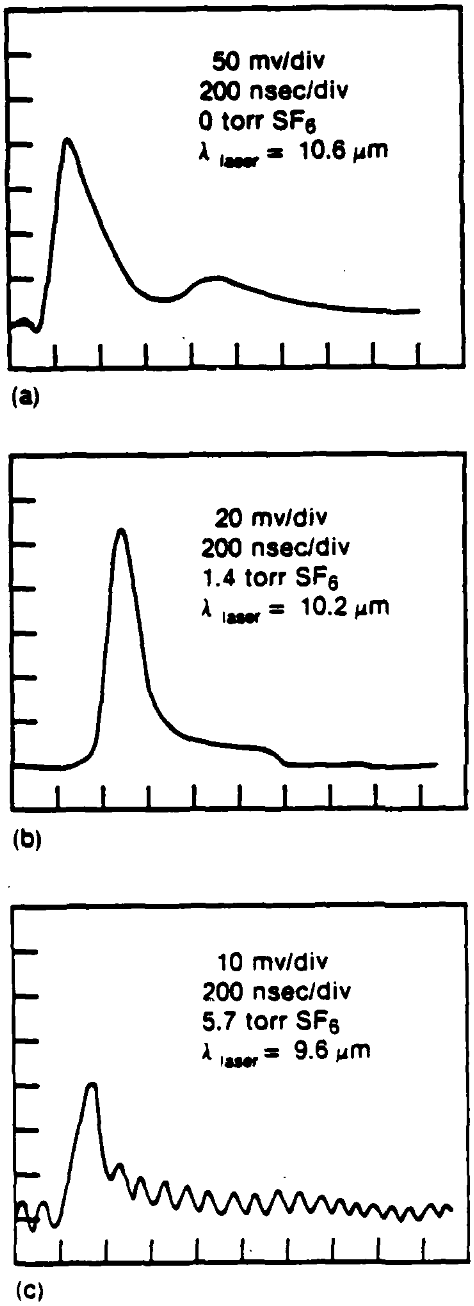

Figure 4: Scope Traces of Laser Pulse With 60cm Gas Cell

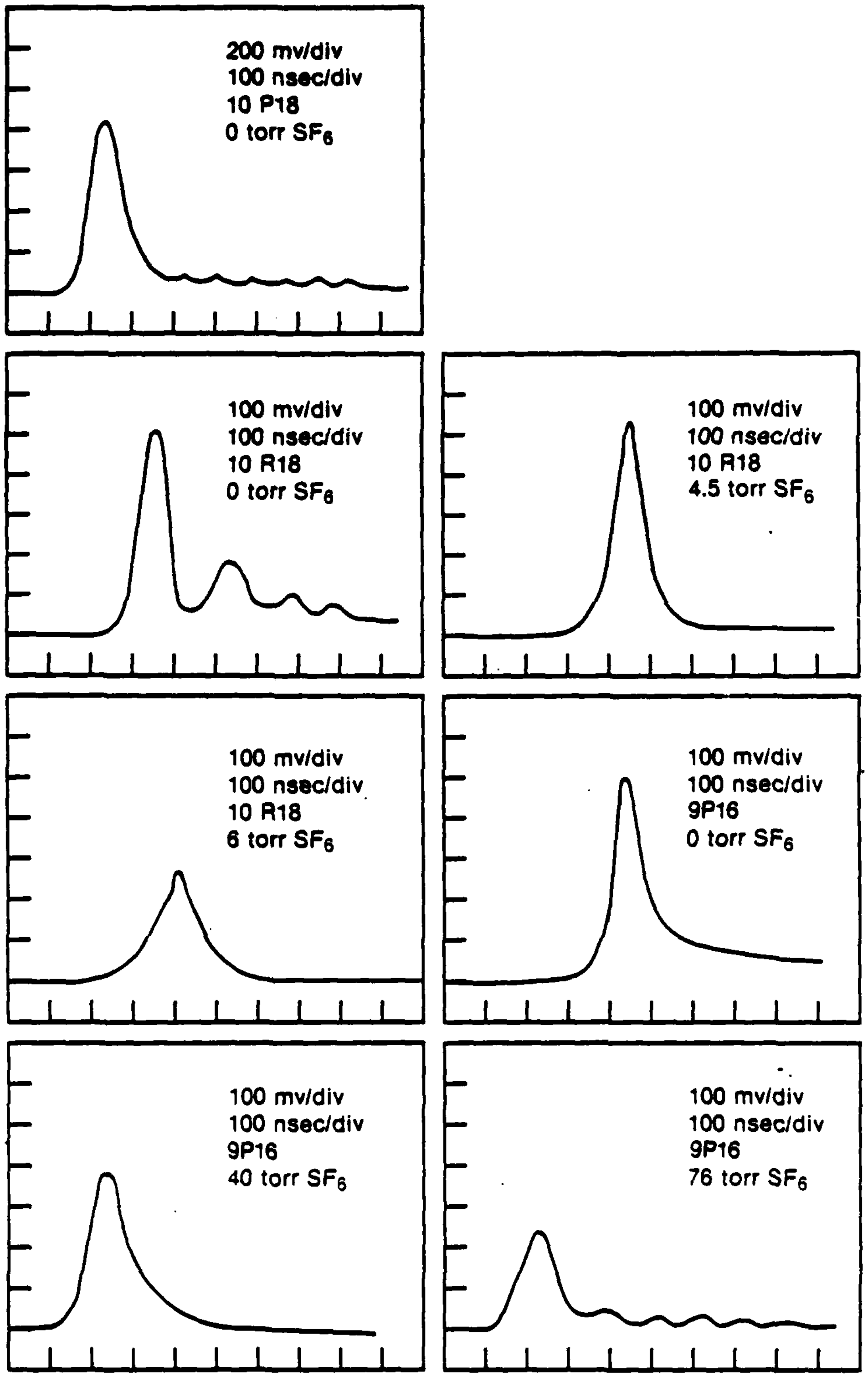

Figure 5: Scope Traces of Laser Pulse With 27cm Gas Cell and Grating

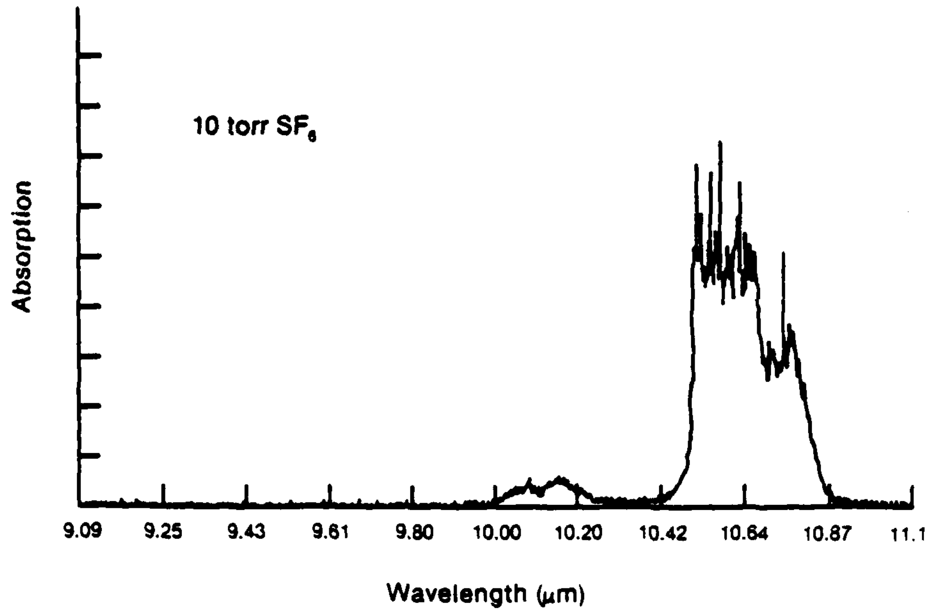

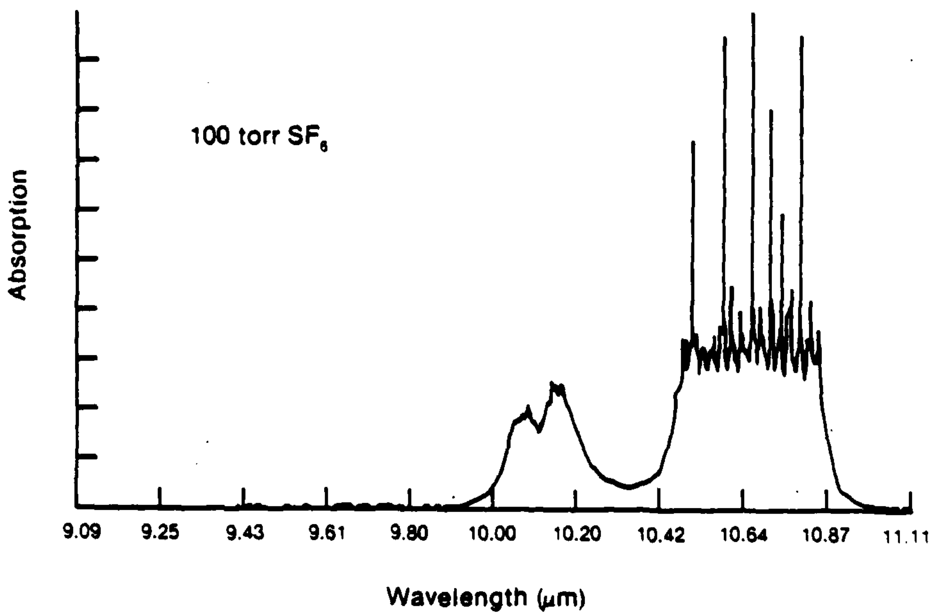

Figure 6: Absorption Spectrum of SF_6 From Perkin Elmer

V. References

1. I. Burak, P. Houston, D. Sutton, and J. Steinfeld, Mechanisms of Passive Q-Switching in CO_2 Lasers, *QE-7*, No. 2, p. 73, 1971.
2. U. Oppenheim and Y. Kaufman, Molecular Saturation of the Criterion for Passive Q-Switching, *IEEE, QE-10*, p. 533, 1974.
3. Y. Kaufman, High Gain in Laser in Passive Q-Switching Operating Criterion, *Applied Optics*, Vol. 15, No. 6, p. 1535, 1976.
4. T. DeTemple and A. Nurmikko, The Dynamics of Single-Mode Operations of High Pressure CO_2 Laser by Means of Saturable Absorbers, *Optics Communication*, Vol. 4, No. 3, p. 231, 1971.
5. R. Fortin, F. Rheault, J. Gilbert, M. Blanchard, and J. Lachambre, Powerful Nanosecond Pulses by Stable Passive Mode Locking of TEA CO_2 Lasers, *Canadian Journal of Physics*, Vol. 51, p. 414, 1973.
6. A. Nurmikko, T. DeTemple, and S. Schawarz, Single-Mode Operation and Mode Locking of High-Pressure CO_2 Lasers by Means of Saturable Absorbers, *Applied Physics*, Vol. 18, No. 4, 1971.
7. A. Yariv, Quantum Electronics, p. 248, John Wiley and Sons, New York, 1975.
8. H. Brunet, Saturation of Infrared Absorption in SF_6, *IEEE Journal of Quantum Electronics*, *QE-6*, No. 11, p. 687, 1970.
9. D. Sutton, I. Burak, and J. Steinfield, Infrared Pulse Transmission in SF_6-He Mixtures, *QE-7*, p. 52, 1971.
10. E. Hinkley, High Resolution Infra-Red Spectroscopy With a Tunable Diode Laser, *Applied Physics Letters*, Vol. 16, No. 9, p. 351, 1970.

Distribution List for NV & EOL Report AMSEL-NV-TR-0056

No. Copies	Addressee
(2)	Defense Technical Information Center ATTN: DDC-TDA Cameron Station (Bldg. 5) Alexandria, VA 22314
(15)	Director Center for Night Vision and Electro-Optics ATTN: AMSEL-RD-NV-L (Mr. Robert Pastel) Fort Belvoir, VA 22060-5677
(1)	Director Center for Night Vision and Electro-Optics ATTN: AMSEL-RD-NV-D Fort Belvoir, VA 22060-5677
(1)	Commander Chemical Research and Development Center ATTN: SMCCR-DDT (Dr. Ray MacKay) Aberdeen Proving Ground, MD 21010-5423
(1)	Naval Weapons Center ATTN: Mr. Robert Hintz Code 31506 China Lake, CA 93555
(1)	Director Harry Diamond Laboratory ATTN: DELHD-TA-L 2800 Powder Mill Road Adelphi, MD 20783
(1)	Honeywell Incorporated Systems and Research Center ATTN: Dr. Fred Faxvog 2600 Ridgway Parkway Minneapolis, MN 55413
(1)	Naval Research Laboratories 4555 Overlook Avenue Coole-6540 Washington, DC 20375-5000
(3)	Director Belvoir RD&E Center STRBE-BPG Ft. Belvoir, VA 22060
(1)	Raytheon Company Equipment Division Electro-Optics Laboratory ATTN: Dr. Greg Osche 528 Boston Post Road Sudbury, MA 01776
(1)	Laser Science Inc. ATTN: Dr. Ali Javan 80 Prospect St. Cambridge, MS 02139
(1)	Westinghouse R&D Center ATTN: Lew Denes 1310 Beulah Road Pittsburgh, PA 15235
(1)	United Technologies Research Center 400 Main Street ATTN: Dr. B. Silverman East Hartford, CT 06108
(1)	Ford Aerospace and Communications Corporation Aeroneutronic Division Ford Road ATTN: Dr. Eli Reisman Newport Beach, CA 92663
(1)	CLS Laser Systems Incorporated 5 Jeffrey Drive ATTN: Dr. Robert DelBoca P.O. Box 767 South Windsor, CT 06074
(1)	GEC Avionics, Inc. 2975 Northwoods Parkway/Norcross P.O. Box 81999 Atlanta, GA 30366
(1)	Texas Instruments Incorporated ATTN: Mr. Carol Taylor P.O. Box 226015 Mail Station 312B Dallas, TX 75266

END

1-87

DTIC